PCCP

Accepted Manuscript

ROYAL SOCIETY OF CHEMISTRY

www.rsc.org/pccp

Systematic Study of the Effect of Molecular Weights of Polyvinyl Alcohol on Polyvinyl Alcohol/Graphene Oxide Composite Hydrogels

Rongrong Xue [a, b], Xia Xin [a, b *], Lin Wang [b], Jinglin Shen [b], Fangrui Ji [b], Wenzhe Li [b], Chunyu Jia [b], Guiying Xu [a, b *]

[a] *National Engineering Technology Research Center for Colloidal Materials, Shandong University, Jinan, 250100, P. R. China*

[b] *Key Laboratory of Colloid and Interface Chemistry (Shandong University), Ministry of Education, Jinan, 250100, P. R. China*

Abstract

Polyvinyl alcohol (PVA) hydrogels have been proposed for use as promising biomaterials in biomedical and tissue engineering, and graphene oxide (GO) has been recognized as a unique two-dimensional building block for various graphene-based supramolecular architectures. In this article, we systematically studied the influence of three kinds of PVA with different molecular weights on the interaction between PVA and GO. Moreover, the effects of GO on the gelation of PVA were also investigated. The native PVA hydrogel, as well as PVA/GO hybrid hydrogels, have been thoroughly characterized by phase behavior study and various techniques including field emission scanning electron microscopy (FE-SEM), Fourier transform infrared (FT-IR) spectroscopy,

[*]Author to whom correspondence should be addressed, E-mail: xinx@sdu.edu.cn.

Phone: +86-531-88363597. Fax: +86-531-88361008

[*]Author to whom correspondence should be addressed, E-mail: xuguiying@sdu.edu.cn

Phone: +86-531-88365436. Fax: +86-531-88564750

thermogravimetric analysis (TGA) and rheological measurements. It can be seen that with the increase of the molecular weight of PVA, the addition of GO can effectively promote the gelation of PVA which can be reflected by a decrease of the critical gel concentration (*CGC*) for PVA/GO hydrogels. Dye adsorption experiments indicate that the toxic dye, i.e., methylene blue (MB), was efficiently entrapped to the PVA/GO xerogels. It is also demonstrated that the gelation of PVA and GO composites can be promoted by different supramolecular interactions, including hydrogen bonding and electrostatic interaction. This work indicates that PVA/GO composite is a good candicate for preparing "super" and "smart" hydrogels and will enlighten further studies on the supramolecular chemistry of PVA, graphene and its derivatives.

Keywords: Hydrogels, polyvinyl alcohol, graphene oxide, phase behavior, hydrogen bonds.

1. Introduction

Polymer hydrogels are three-dimensional networks of cross-linked polymer chains swollen with water. They have a wide array of applications, such as drug delivery systems, biosensors, and sustained drug-release [1-4]. They are formed by cross-linking of polymer chains by covalent bonds, hydrogen bonding, van der Waals interactions, or physical entanglements [5]. However, the mechanical properties (toughness, crack resistance) of the hydrogels are often poor, which limits their applications. Recently, much research has been devoted to improve the mechanical performance of the hydrogels [6, 7]. Construction of composite hydrogels with nanofillers such as silica, clay, and carbon nanotubes is considered to be an effective way to enhance the mechanical strength and toughness of the hydrogels [8-11].

As a new kind of carbon material, graphene, a single-layered and two-dimensional lattice, was first reported in 2004 [12] and has been widely investigated because of its unique mechanical, quantum and electrical properties [13-15]. Graphene oxide (GO), a modified form of graphene, consists of a two-dimensional (2D) sheet of covalently bonded carbon atoms bearing various oxygen functional groups (e.g. hydroxyl, epoxide, and carbonyl groups) on their basal planes and edges. Therefore, GO is hydrophilic and can be readily dispersed in water as individual sheets to form stable colloidal suspensions [16, 17]. Meanwhile, these oxygen-containing groups impart GO sheets with the function of strong interaction with polar small molecules or polymers to form GO intercalated or exfoliated composites [18, 19]. Thus, graphene oxide (GO) has been recognized as a unique 2D building block for various graphene-based supramolecular architectures. Recently, single-stranded DNA was also found to be a good cross-linker for preparing a GO/DNA composite hydrogel, in which π-π interaction was the dominant driving force [20].

Polyvinyl alcohol (PVA) can form intriguing hydrogel, which has been proposed as promising biomaterials in biomedical and tissue engineering for repairing diseased or damaged articular cartilages, meniscuses and tendons due to its excellent biocompatibility and water absorption abilities [21]. But its poor mechanical and water-retention properties have hindered its development and application [22]. Incorporation of nanomaterials such as GO into PVA hydrogels is a way to improve their mechanical properties. Liu et al. used GO as an excellent nanofiller and prepared GO/PVA composite hydrogels by a freeze/thaw method. They demonstrated that the mechanical properties of the GO/PVA hydrogels were significantly improved. Compared to pure PVA hydrogels, a 132% increase in tensile strength and a 36% improvement of compressive strength were achieved with the addition of 0.8 wt% of GO, which suggests an excellent load transfer between the GO and the PVA matrix [22]. Shi et al. demonstrated that GO sheets were able to form composite hydrogels with PVA where GO sheets acted like 2D macromolecules [23, 24]. The formation of the hydrogels relies on the assembly of GO sheets and the cross-linking effect of PVA chains. Moreover, they revealed that the GO/PVA hydrogels exhibited pH-induced gel–sol transition,which can be used for loading and selectively releasing drugs at physiological pH. Huang et al. added 0.7 wt% GO into a PVA matrix and the resulting GO/PVA composite had a 76% increase in tensile strength and a 62% improvement in Young's modulus [25].

In this article, three kinds of PVA with varying molecular weights were used to give a systematic study of the interaction between PVA and GO. The effect of GO on the gelation of PVA was also explored. We characterized this performance through phase behavior observation, field emission scanning electron microscopy (FE-SEM), Fourier transform infrared (FT-IR) spectroscopy, thermogravimetric analysis (TGA) and rheological measurements. This work demonstrates another

example for the preparation of high-performance polymer nanocomposties by using GO as a nanofiller. It can be expected that PVA/GO hydrogels with largely improved mechanical properties may play a more important role in biochemical and electrochemical applications.

2. Experiments

2.1 Materials

Three kinds of Poly (vinyl alcohol) (PVA) with varying molecular weights were purchased from Sigma-Aldrich (Shanghai) Trading Co, Ltd. They are respectively expressed as high PVA (h-PVA), middle PVA (m-PVA) and low PVA (l-PVA) for convenience. Their properties are shown in table 1. Graphene oxide (diameter: 0.5~5 μm; thickness: 0.8~1.2 nm; single layer ratio: ~99%; purity: ~99%) was obtained from Nanjing XFNANO Materials Tech Co., Ltd and was used as received. Water used in the experiments was triply distilled by a quartz water purification system.

Table 1 Properties of PVA used in the work

PVA	Repeat unit number of -$CH_2CH(OH)$	Mw	Alcoholysis degree
High PVA (h-PVA)	3318-4227	146,000-186,000	99+%
Middle PVA (m-PVA)	1932-2818	85,000-124,000	99+%
Low PVA (l-PVA)	705-1136	31,000-50,000	98-99+%

2.2 Preparation of samples

Preparation of PVA solution: A certain amount of PVA was added to deionized water and stirred continuously at 95 °C for a week. Then the samples were kept at 20□ for two weeks before characterization.

Preparation of GO dispersion: The desired amount of dried GO was exfoliated and dispersed in

deionized water by sonication for 4 h. In this way, we can make a homogenous brown dispersion of GO for preparing the PVA/GO composite hydrogels.

Preparation of PVA/GO composite hydrogels: GO dispersion and PVA solution was mixed together at a certain ratio. The mixture was shaken violently for 50s and further treated by sonication for 20 min. The composite gels were kept at 20□ for two weeks before characterization.

2.3 Instruments and characterizations

For transmission electron microscopy (TEM) observations, about 5 μ L of solution was placed on a TEM grid and the excess solution was wicked away with filter paper. The copper grids were freeze-dried and observed on a JEOL JEM-100 CXII (Japan) at an accelerating voltage of 80 kV. For field-emission scanning electron microscopy (FE-SEM) observations, a drop of sample solution was placed on a silica wafer to form a thin film. The wafers were freeze-dried in a vacuum extractor at −55 °C and were observed on a JSM-6700F. FTIR spectrum of the freeze-dried hydrogel powder for KBr test was recorded on a VERTEX-70/70v spectrometer (Bruker Optics, Germany). DSC measurements were performed by a DSC Q10 V9.7 Build 291 in a DSC standard cell FC. An empty aluminum pan was used as a reference. The samples were equilibrated at 20.0 ± 0.1 °C for 10 min and then heated to 230 °C at a heating rate of 3 °C min^{-1}. TGA data were collected using a Universal V3.6 TA Thermal Analysis Q5000 system. The sample was placed in a platinum crucible and heated under a flow of N_2 from ~50 ºC to 800 ºC at a heating rate of 10 ºC min^{-1}.

The rheological properties of hydrogels were measured at 20.0 ± 0.1□ with an Anton Paar Physica MCR 302 rheometer (cone and plate geometry of 25 mm in diameter with the cone gap equal to 0.106 mm). Frequency spectra were conducted in the linear viscoelastic region of the samples determined from dynamic strain sweep measurements. The dynamic stress sweep from 0.1

to 100 Pa was carried out at an angular frequency of 1Hz, the frequency sweep was performed over the frequency range of 0.01-100 Hz at a fixed stress of 1Pa.

3. Results and discussion

3.1 Dispersion of GO

Firstly, we prepared GO dispersion in deionized water by sonication. TEM image shows that GO contains several graphitic layers, some of which fold to induce wrinkles (Figure 1). For GO, oxygen-containing functional groups including hydroxyls, epoxides, diols, ketones and carboxyls significantly alter the van der Waals interactions between the graphitic layers and impart GO with desired water solubility [25-28]. Thus, a GO sheet can be regarded as a single- or few-layered graphite that brings various hydrophilic oxygenated functional groups and it can be dispersed in water to form a stable colloidal dispersion for several months with no precipitation occurring [29]. It was also believed that the electrostatic repulsion between GO sheets, resulting from their ionized carboxyl groups, prevented their aggregation in aqueous medium [30].

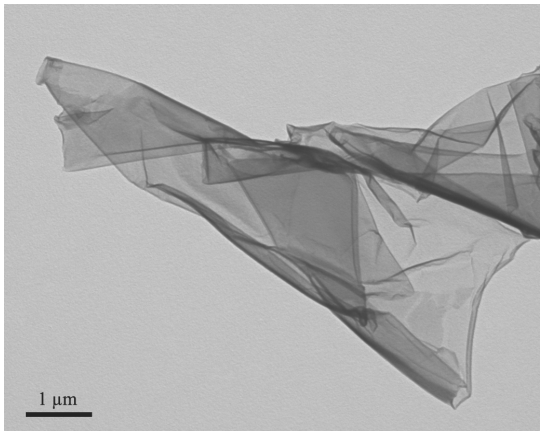

Figure 1 A typical TEM image of water-dispersed (5 mg mL^{-1}) graphene oxide.

3.2 Phase behavior of PVA/GO mixed system

Phase behavior study on PVA/GO mixed system was performed to determine the conditions for the formation of PVA/GO hydrogels. PVA, which is also water-soluble due to its many hydroxyl groups, was expected to homogenously co-dispersed with graphene at the molecular level. Furthermore, potential H-bonding between GO and PVA could lead to enhanced interfacial adhesion and mechanical performance of the nanocomposite [31]. Therefore, the addition of PVA can increase the bonding force between GO sheets and consequently promote gelation. Also, the molecular weights and the molar masses of the PVA are expected to be able to influence the gelation process of GO hydrogels.

To get more details, three kinds of PVA with varying molecular weights were selected to tune the interaction between PVA and GO. It can be seen from Figure 2 (A-D) when the concentration of GO (C_{GO}) is fixed at 1 mg L^{-1} Figure 2 (D) and 3 mg L^{-1} Figure 2 (C), respectively, the samples can not form hydrogels within the investigated concentrations of m-PVA ($c_{m\text{-}PVA}$). Instead, solutions which can flow under gravity formed. When c_{GO} is increased to 5 mg mL^{-1} Figure 2 (B), however, formation of hydrogels was induced when $c_{m\text{-}PVA}$ is higher than 0.25 mg mL^{-1}. Thus, c_{GO} is crucial for the formation of a three-dimensional (3D) GO infinite network. If c_{GO} is lower than the critical gel concentration (*CGC*) of the GO/polymer hydrogel, the intercontacts between GO sheets are insufficient for forming a stable network even at the presence of a cross-linker (i.e., PVA).

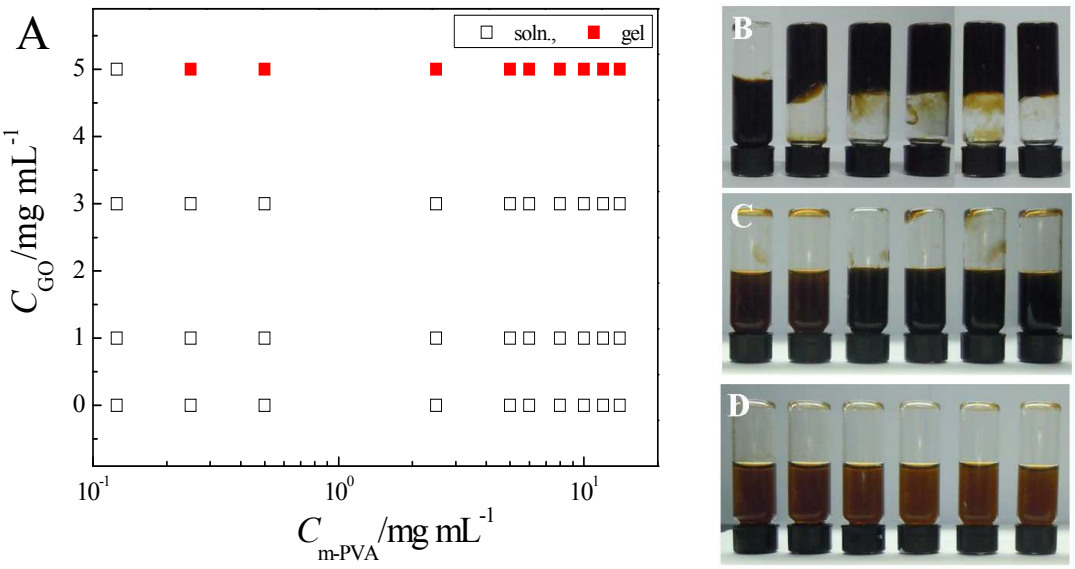

Figure 2 (A) Phase behavior of m-PVA/GO mixed system after equilibrated at 20.0 ± 0.1ºC for at least 2 weeks. Photographs of 5 mg L^{-1} (B) 3 mg L^{-1} (C) and 1 mg L^{-1} (D) of GO solutions mixed with different concentrations of m-PVA. $c_{m\text{-}PVA}$ is (from left to right) 0.125, 0.25, 0.5, 2.5, 5 and 8 mg mL^{-1}, respectively.

The results reported by Shi et al. show that gelation occurs as the GO network in solution is reinforced by enhancing the bonding force or weakening the repulsion force [24]. According to the analyses described above, the addition of a cross-linker can increase the bonding force between GO sheets and consequently promote gelation. In theory, the molecular weight of PVA can affect its ability of promoting gelation of GO. Thus, we fixed the concentration of GO (5 mg mL^{-1}) and investigated the influence of the molecular weight of PVA on the PVA/GO hydrogel formation. We conjecture that the *CGC* of three kinds of PVA/GO hydrogels maybe decrease gradually with the increase of the molecular weight of PVA.

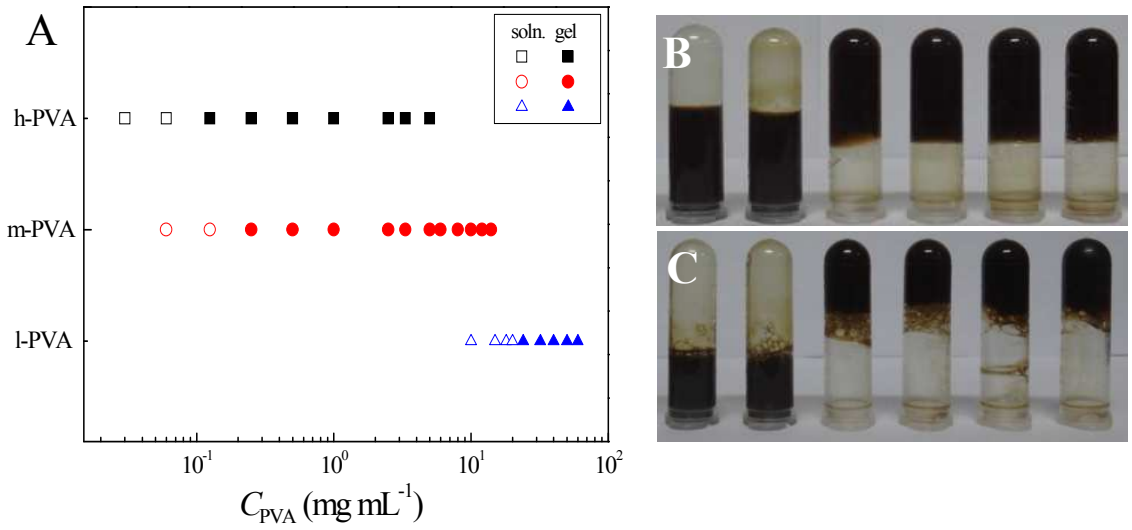

Figure 3 (A) Influences of the molecular weight and concentration of PVA on the phase behavior of PVA/GO mixed system (c_{GO}=5 mg mL^{-1}) after equilibrated at 20.0 ± 0.1ºC for at least 2 weeks. Photographs of 5 mg mL^{-1} GO solutions mixed with h-PVA (B) and l-PVA (C), respectively. The concentration of PVA (from left to right) is (B) 0.03, 0.06, 0.125, 0.25, 0.5, 1 mg mL^{-1} and (C) 18, 20, 24, 28, 32, 36 mg mL^{-1}, respectively. The samples were stored at 20.0 ± 0.1ºC for at least two weeks before the photos were taken.

The phase behavior of h-PVA/GO, m-PVA/GO and l-PVA/GO mixed systems (c_{GO} = 5 mg mL^{-1}) is shown in Figure 3 (A) and the photographs of typical samples are given in Figure 3 (B, C). It can be seen that *CGC* of PVA/GO hydrogels really decreased with the increase of the molecular weight of PVA. $CGC_{h\text{-}PVA}$, $CGC_{m\text{-}PVA}$ and $CGC_{l\text{-}PVA}$ is determined to be 0.125 mg mL^{-1} (Figure 3 B), 0.25 mg mL^{-1} (Figure 2 B) and 24 mg mL^{-1} (Figure 3 C), respectively. Thus, it can be concluded that the higher molecular weight of PVA, the lower concentration of PVA to induce the formation of PVA/GO hydrogel. It can be inferred that with the increase of the molecular weight of PVA, both the number of hydrogen bonds formed between PVA and GO and the number of the GO layers linked by the PVA molecules at the same concentration of PVA increases due to the longer length of

the PVA molecules, which can effectively promote the gelation of GO.

Microstructures of the self-assembled structures

The micro-morphology of the hydrogel is also crucial for the analysis of the formation mechanism of the system. The lyophilized GO dispersion shows a 3D network composed of GO sheets (Figure 4 A and B). It is reasonable to conclude that a loose GO network existed in the freeze-dried 5 mg mL^{-1} GO solution owing to a force balance between electrostatic repulsion and binding interactions (hydrogen bonding, hydrophobic effect, etc.).

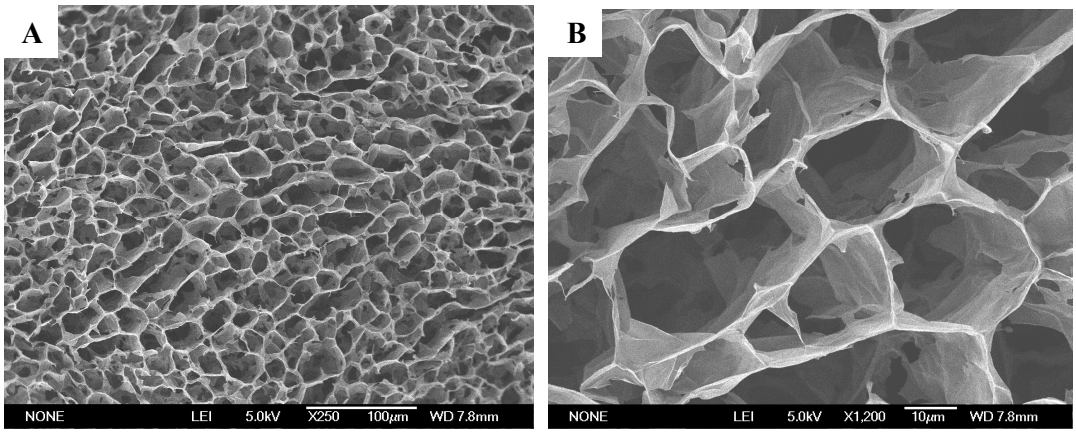

Figure 4 SEM images of (A) freeze-dried 5 mg mL^{-1} GO solution, (B) a local partial enlarged image of (A).

Then, we choose m-PVA/GO system as the representative to observe their morphology. It can be seen that the sheet layer of freeze-dried 8 mg mL^{-1} m-PVA is unordered and has relatively large size (Figure 5 A). When 5 mg mL^{-1} GO was incorporated, the hydrogels formed. PVA can form hydrogen bonds with adjacent GO sheets, providing an additional bonding force for the gelation of GO. All the m-PVA/GO composite hydrogels show 3D networks with a morphology similar to that of pure GO, indicating that the addition of m-PVA did not change the conformation of GO sheets. However, it can be observed that as the concentration of m-PVA increased from 2.5 to 8 mg mL^{-1},

the network of the samples become thicker and larger (Figure 5 B-D). Moreover, during the process of SEM test, it can be observed that at high magnification, m-PVA itself was easily destroyed by the electron beam. Interestingly, since GO nanosheets are thermal conductors, to some extent the m-PVA loaded with GO can suffer the bombardment of the electron beam.

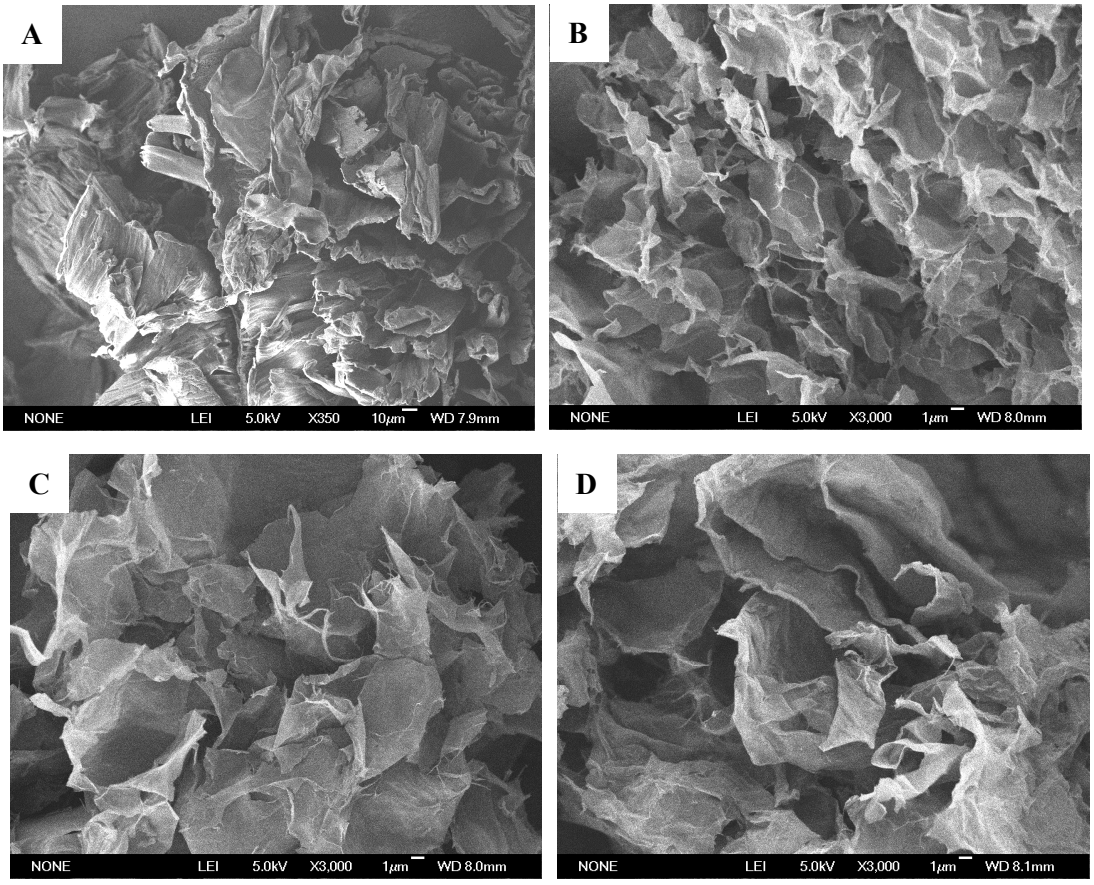

Figure 5 SEM images of freeze dried samples: (A) 2.5 mg mL^{-1} m-PVA; (B) 2.5 mg mL^{-1} m-PVA/5 mg mL^{-1} GO; (C) 5 mg mL^{-1} m-PVA/5 mg mL^{-1} GO; (D) 8 mg mL^{-1} m-PVA/5 mg mL^{-1} GO.

Rheological properties of PVA/GO hydrogels

The viscoelastic properties of the hydrogels were examined in a dynamic stress environment by a rheometer [5]. Before carrying out any oscillatory measurements, each sample should be checked to ensure that it is within the linear viscoelastic region, where G′ and G″ are independent of the

applied stress. The influences of the concentration of m-PVA on the rheological properties of m-PVA/GO hydrogels with a GO concentration of 5 mg mL^{-1} were investigated by the stress sweep at a fixed frequency of 1.0 Hz (Figure 6). It can be seen that for all the samples G′ is always higher than G″ within the investigated stress range, which reveals the elasticity of the hydrogels (Figure 6 A). From Figure 6 A, it can be also seen that both G′ and G″ remain nearly constant with the increase in stress (τ) until the yield-stress value (τ_c, the stress at the inflection point) is reached, indicating considerable mechanical stability of the composites. When $c_{m\text{-}PVA}$ < 6 mg mL^{-1}, the intensity of G′ and G″ first increases continuously with $c_{m\text{-}PVA}$, indicating that the strength of the m-PVA/GO hydrogels was enhanced. However, adding excess m-PVA decreases the strength of m-PVA/GO hydrogels (Figure 6 B).

Then, the frequency sweep was used to determine the viscoelasticity of the hydrogels. Similar with the phenomenon observed in stress sweep, G′ is higher than G″ over the studied frequency range, indicating that the hydrogels exhibit "solid-like" behavior with an dominant elastic property (Figure 7 A-E), which is general in gels [32, 33]. Both G′ and G″ first increase with the increase of $c_{m\text{-}PVA}$, which should be ascribed to the more rigid networks of the hydrogels caused by more entanglements with increasing fibril density [34]. Then both G′ and G″ decrease with further increase of $c_{m\text{-}PVA}$ (5 mg mL^{-1}) as shown in Figure 7 F. During the formation of GO/PVA hydrogels, GO sheet provides the structural basis for the formation of gel network and PVA acts as a cross-linker in PVA/GO hydrogels which makes strong hydrogen bonds between PVA molecular chain and GO layers. PVA molecule can attach to the GO sheets and also interact with adjacent GO sheets. With increasing amount of PVA, this interaction was further enhanced and thus the gel strength was also enhanced. However, at large amount of PVA, PVA chains entangle by themselves,

which decreases the ability of PVA to connect GO layers. Moreover, the addition of PVA can also hinder the interaction between GO layers, thus, the strength of network weakened and the gel strength decreased.

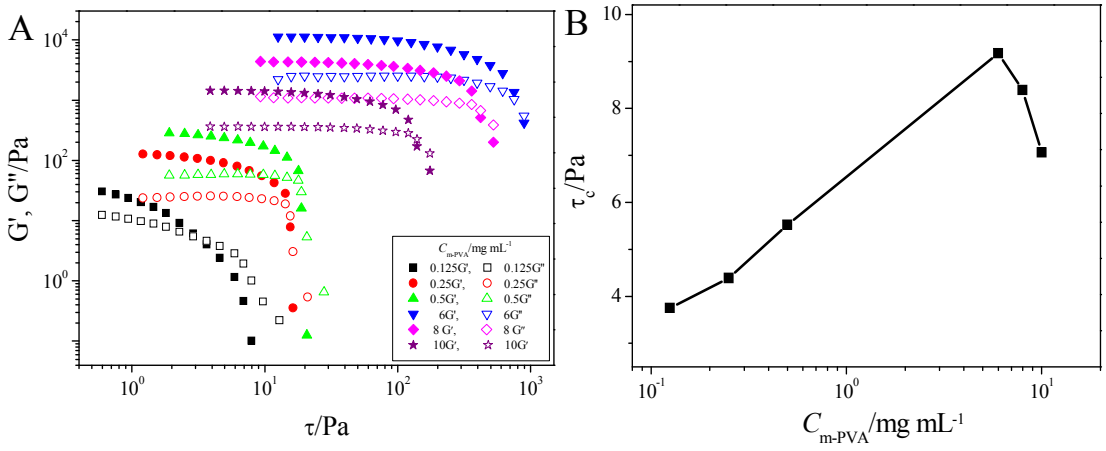

Figure 6 (A) Elastic modulus (G′) and viscous modulus (G″) of different concentration of m-PVA/5 mg mL^{-1} GO hydrogels as a function of the applied stress at a constant frequency (1.0 Hz); (B) Variation of τ_c as a function of the concentration of m-PVA.

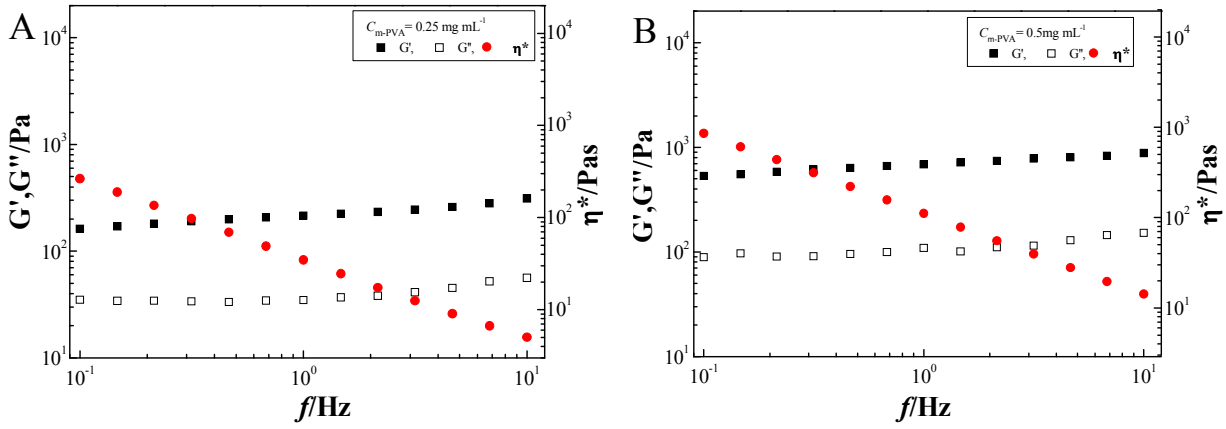

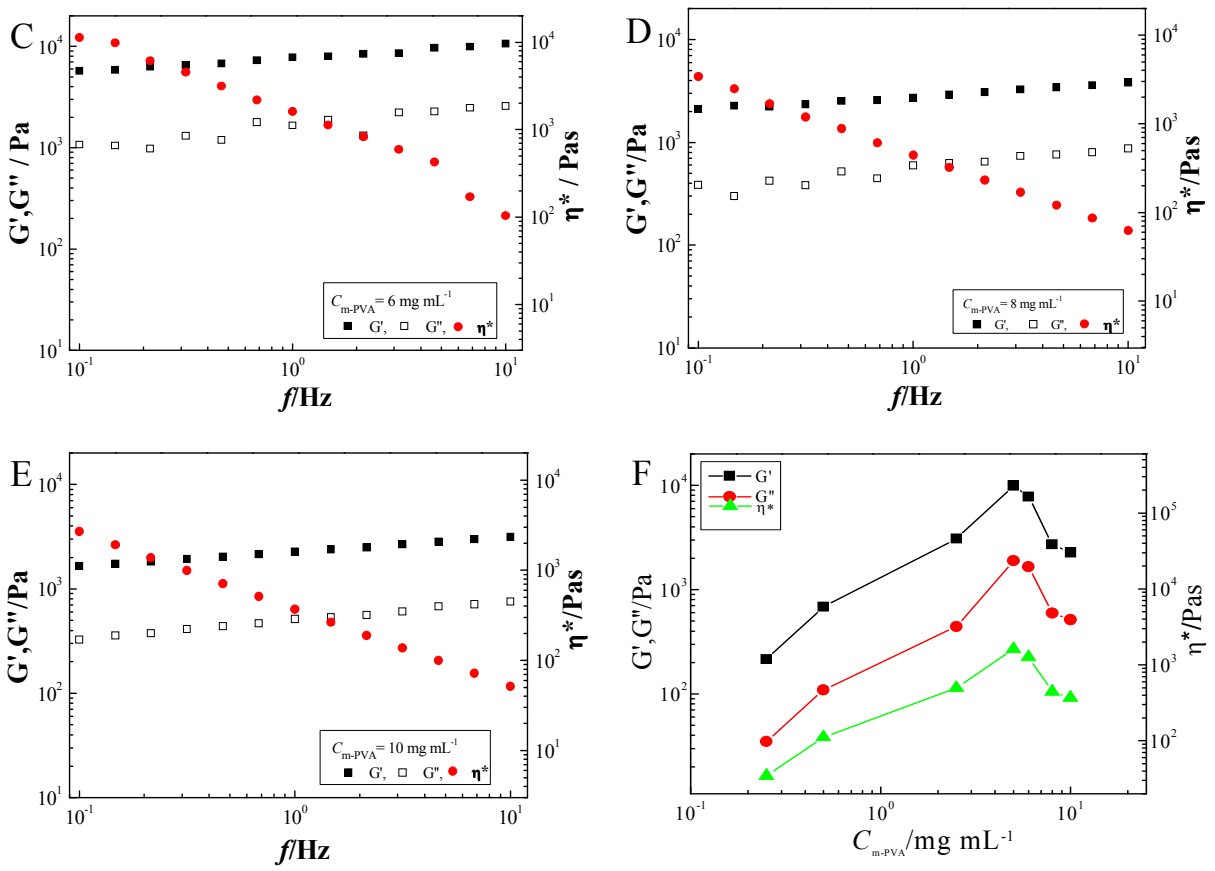

Figure 7 Oscillatory rheological measurements of m-PVA/GO hydrogels formed by 5 mg mL^{-1} GO with (A) 0.25 mg mL^{-1}, (B) 0.5 mg mL^{-1}, (C) 6 mg mL^{-1}, (D) 8 mg mL^{-1} and (E) 10 mg mL^{-1} m-PVA. (F) Variation of G′, G″ and η^* of m-PVA/GO hydrogels as a function of the concentration of m-PVA at the presence of 5 mg mL^{-1} GO.

The variations of G′, G″ and η^* of PVA/GO hydrogels as a function of the concentration of $c_{l\text{-PVA}}$ (Figure 8 A) and $c_{h\text{-PVA}}$ (Figure 8 B) at the presence of 5 mg mL^{-1} GO have the same tendency as that found in m-PVA. The highest values of G′, G″ and η^* appeared at 36 and 1 mg mL^{-1} l-PVA and h-PVA, respectively. It has been demonstrated that GO or graphene can act as crystal nucleus for PVA [35, 36], which has two effects on the non-isothermal crystallization process of PVA: one is the nucleation effect which could accelerate the crystallization rate and the other is the impeding effect which could slower the crystallization rate by retarding the transport of molecules to the

growing crystals [37, 38]. Thus, the physical crosslink within the crystal domains can promote the gelation especially at high PVA concentrations. Moreover, it can be seen that the concentration of PVA at which the PVA/GO hydrogels with the highest strength formed decreases with the increase of the molecular weight of PVA, which is consistent with the phase behavior study.

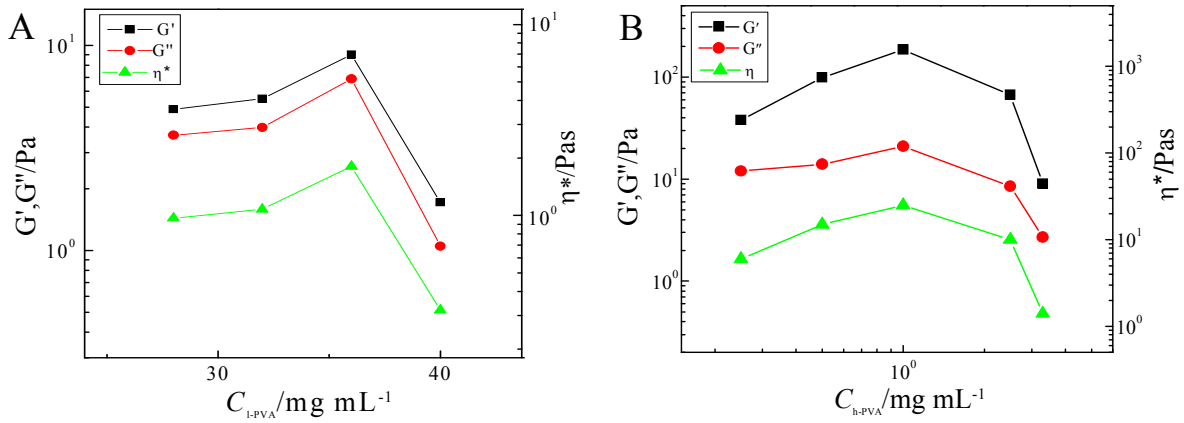

Figure 8 Variation of G′, G″ and η^* of PVA/GO hydrogels as a function of $c_{l\text{-}PVA}$ (A) and $c_{h\text{-}PVA}$ (B) molecular weight of PVA at the presence of 5 mg mL^{-1} GO.

FT-IR results

FT-IR spectroscopy is a powerful method for characterizing the interactions within supramolecular assemblies and is powerful enough to detect the hydrogen bond within the region of 1800-400 cm^{-1} [39]. As shown in Figure 9, in the spectrum of GO, the peak at 1730 and 1630 cm^{-1} are characteristics of the C=O stretch of the carboxylic group on the graphene oxide and deformations of the O-H bond in water, respectively [40]. For all the samples, the wide peak at about 3442 cm^{-1} is well-known for symmetric and antisymmetric O-H stretching modes for PVA and GO. It can be also seen that the asymmetric and symmetric methylene stretching bands are located at 2933 and 2860 cm^{-1}, respectively. Moreover, the peak at 1093 cm^{-1} is in agreement with the stretching vibration of C-O bond and the weak peaks at 1419 cm^{-1} are correlated with the

bending vibration of O-H for PVA and GO. From FTIR spectra, it can be concluded that the oxygen-containing groups on the GO surface maybe interact with the PVA molecules through hydrogen bonding. Moreover, it also can be concluded that changing the concentration of PVA or GO only has a limited effect on the FT-IR spectra.

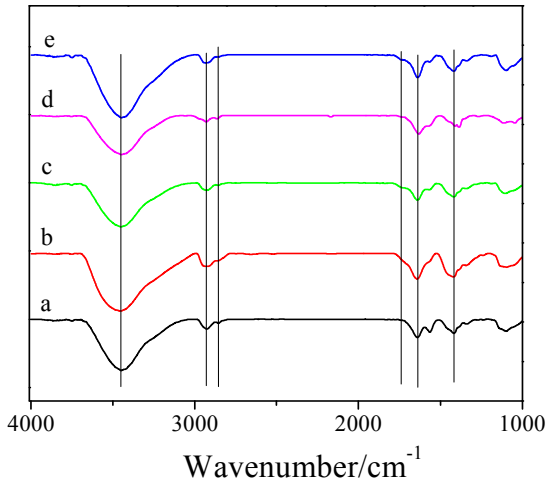

Figure 9 (A) FT-IR spectra of freeze-dried samples composed of (a) 8 mg mL^{-1} m-PVA, (b) 8 mg mL^{-1} m-PVA/1 mg mL^{-1} GO; (c) 8 mg mL^{-1} m-PVA/3 mg mL^{-1} GO; (d) 8 mg mL^{-1} m-PVA/5 mg mL^{-1} GO; (e) GO.

Thermal Properties of PVA/GO Composite Hydrogels (DSC and TGA analysis)

It is interesting to note that the mechanical performance was not the only aspect of the hybrid hydrogels which has been enhanced by the addition of GO. The thermal stability of the composite was also mildly increased even with low loadings of GO. That means the glass-transition temperature (T_g) of PVA is affected by the mobility of PVA chains. Differential scanning calorimetry (DSC) was used to investigate T_g of the PVA/GO nanocomposites. It can be seen that the melting peaks had similar patterns and were in the same range of 100-130 ºC (Figure 10 A). With the increase of the concentration of PVA from 0.06 mg mL^{-1} to 5 mg mL^{-1}, T_g increases gradually from

112.4 ºC to 121.8 ºC. The increase in T_g can be ascribed to an effective attachment of PVA to the GO sheets that constrains the segmental motion of the PVA chains by hydrogen bonding. Thermogravimetric analysis (TGA) results for pure PVA and PVA/GO nanocomposite with 5 mg mL^{-1} GO are shown in Figure 10 B. Both pure PVA and the nanocomposite decompose in a two-step process. TGA curve of the nanocomposite shifted toward a higher temperature compared to that of pure GO but somewhat lower than that of pure PVA. The final rest of the weight of PVA/GO nanocomposites is between pure PVA and GO. These results also indicate that addition of GO at low concentrations somewhat improved the thermal stability of the nanocomposites.

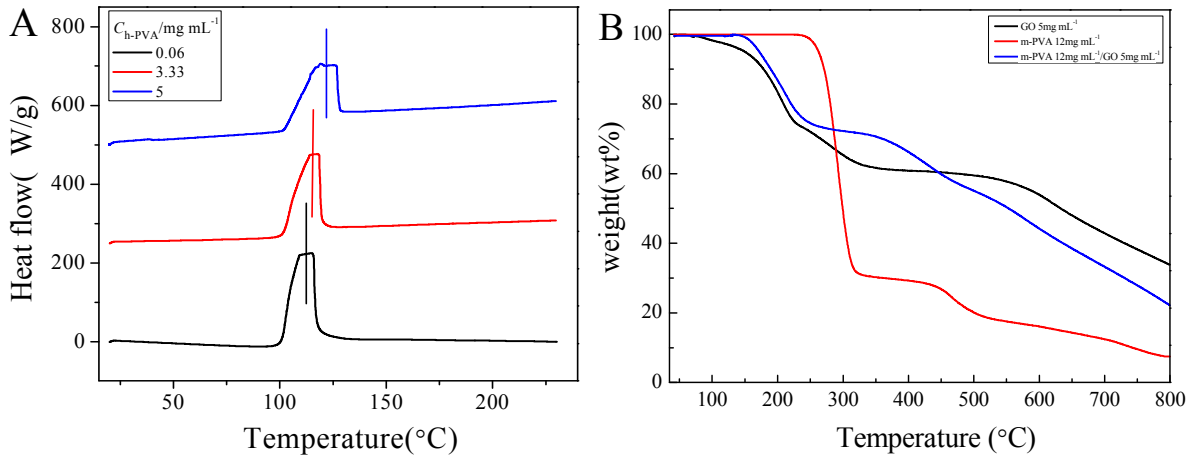

Figure 10 (A) Melting peaks of m-PVA/GO nanocomposites with GO loadings of 5mg mL^{-1}. (B) TGA curves of m-PVA, GO and m-PVA/GO nanocomposite with 5 mg mL^{-1} GO loading.

Formation Mechanism of the PVA/GO Hydrogels

Combined with the experimental results presented above, it can be concluded that the oxygen-containing groups and negative charges on the GO surface can interact effectively with the PVA molecules through hydrogen bonding. Moreover, the large aspect ratio of the graphene sheets is also favorable to stress transfer which means that PVA/GO hydrogels can withstand greater stress.

The compatibility and strong interaction between GO and the PVA matrix greatly enhances the dispersion of GO sheets on the molecular scale in PVA matrix as well as the interfacial adhesion of PVA chains to GO [41], which significantly changes the phase behavior and increases the mechanical properties of the nanocomposites by modifying their microstructures. A reasonable formation mechanism of the PVA/GO hydrogels is given in Scheme 1.

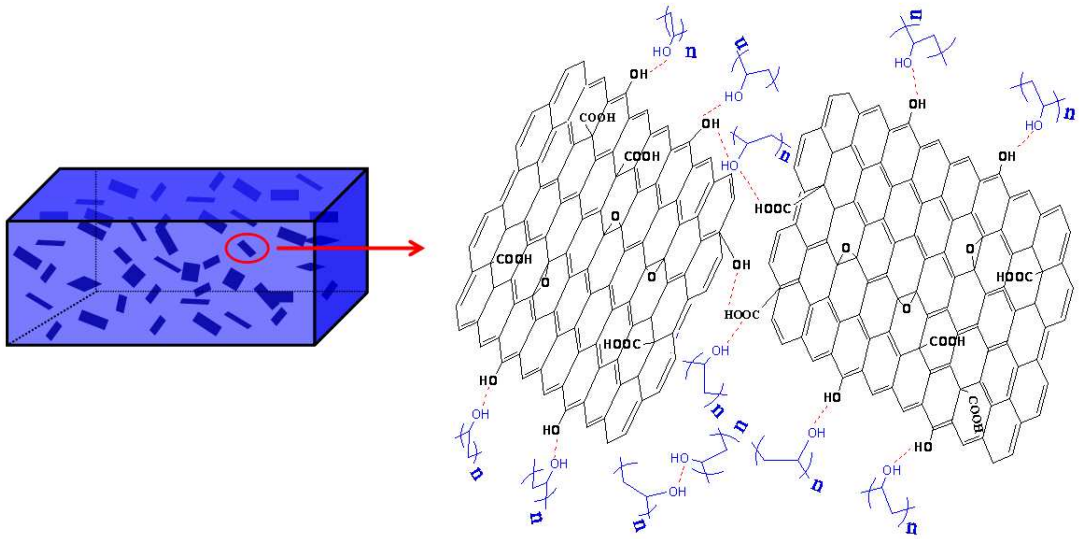

Scheme 1. Schematic representation of the network structure of PVA/GO hydrogel.

Dye Adsorption

Methylene blue (MB) is an aromatic heterocyclic compounds and it is clinically used as the antidote of cyanide and nitrite poisoning and also a photosensitizer to inactivate the virus in single bag of fresh plasma [42]. Therefore, MB is inevitably present in the medical sewage. In addition, medical sewage also contains a variety of biological toxicity or "carcinogenic, teratogenic, mutagenic" properties of drugs, which can induce the emergence of resistant bacteria and cause the damage of water biota [43]. At the same time, the commonly used synthetic drugs always contain the aromatic molecular structure which is difficult to be biodegraded. Therefore, the effective

treatment of sewage is of significance to human health and the environment. Graphene oxide which is with large specific surface properties may have a very bright application prospect in the treatment of medical sewage [44, 45].

In this paper, we did a preliminary attempt on the adsorption of MB using our hydrogel. For a typical process, 0.002 g of freeze-dried samples from 5 mg mL^{-1} aqueous solution was submerged in 3 mL of solution containing 0.05 mmol L^{-1} MB and then left undisturbed. It can be seen that m-PVA can not adsorb MB even after total dissolution (Figure 11 A). GO can adsorb MB, but the process is slow and the bluish-black solution became clear after 240 min. In contrast, the dye molecules were efficiently entrapped to m-PVA/GO xerogel and the bluish-black solution became clear within 60 min (Figure 11 C). The concentration variation of MB was monitored by UV-vis spectra (Figure 11 D). It is clearly seen that the concentration of MB decreased sharply after the addition of the xerogel and the absorption bacame constant after 60 min. As already demonstrated by others [46], for such MB removal, the adsorption follows a second-order kinetic model, i.e., the Morris-Weber model, and the controlling step of adsorption is the intraparticle diffusion. MB adsorption isotherm follows Freundlich model and is heterogeneous. Moreover, the desorption studies they did indicate that the interaction between PVA hydrogels and MB are both physisorption and chemisorption. From a viewpoint of physical interaction, we think that the adsorption may be driven by electrostatic interaction, hydrogen bonding and π-π conjugation between MB and PVA/GO nanocomposites. It can be seen that due to the efficient adsorption of the toxic dye molecules, this hydrogel system can be used as an environmentally friendly water-purifying agent [32].

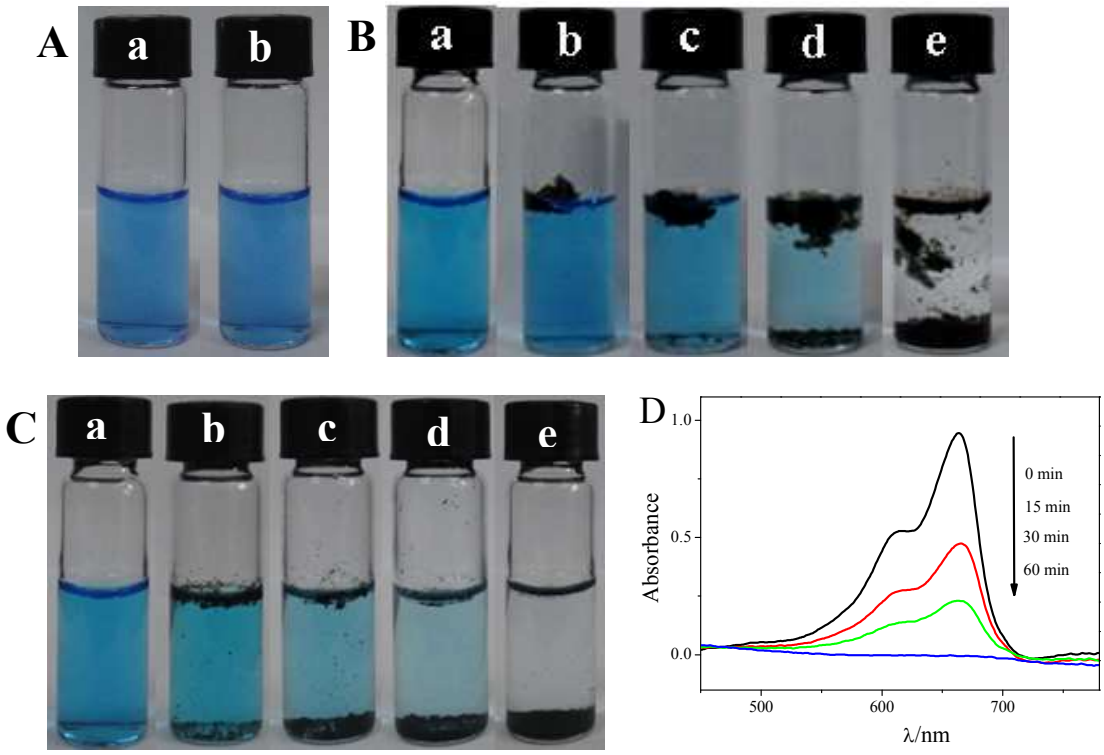

Figure 11 (A) 0.05 mmol L^{-1} MB aqueous solution without (a) and with (b) freeze-dried m-PVA (0.002 g). (B) MB aqueous solution without (a) and with (b-e) freeze-dried GO (0.002 g) at 0 (b), 60 (c), 120 (d) and 240 (e) min, respectively. (C) MB aqueous solution without (a) and with (b-e) freeze-dried m-PVA/GO xerogel (0.002 g) at 0 (b), 15 (c), 30 (d) and 60 (e) min, respectively. (D) UV-vis spectra of MB aqueous solution with m-PVA/GO xerogel at different time.

Conclusions

The influence of three kinds of PVA with varying molecular weights on the interaction between PVA and GO were investigated. The addition of GO can induce PVA solution to form PVA/GO hydrogels. It is observed that GO is dispersed on a molecular scale in the PVA matrix and some interactions occur between PVA matrix and GO sheets. It also can be seen that the increase of the molecular weight of PVA can effectively promote GO for the gelation of PVA which can be

reflected by a decrease of the CGC for PVA/GO hydrogels. With the addition of PVA, the viscoelastic properties of the GO-based PVA/GO hydrogels are significantly improved. Hydrogen bonding between GO sheets and PVA chains is believed to be responsible for the formation of the hydrogel. The PVA/GO nanocomposite shows a variety of petential applications, as illustrated by dye adsorption. Other applications in drug delivery and bioengineering can be also well expected.

Acknowledgement

We gratefully acknowledge financial support from the National Natural Science Foundation of China (21203109), the Special Program for Major Research of the Science and Technology, China (Grant Nos. 2011ZX05024-004-08) and Ji'nan Youth Science and Technology Star Program (2013040).

References

[1] N. A. Peppas, J. Z. Hilt, A. Khademhosseini and R. Langer, *Adv. Mater.*, 2006, **18**, 1345-1360.

[2] Y. Qiu, K. Park, *Adv. Drug Delivery Rev.*, 2001, **53**, 321-339.

[3] N. S. Satarkar, D. Biswal, J. Z. Hilt, *Soft Matter*, 2010, **6**, 2364-2371.

[4] S. Das, F. Irin, L. Ma, Sanjoy K. Bhattacharia, Ronald C. Hedden, and Micah J. Green, *ACS Appl. Mater. Interfaces*, 2013, **5**, 8633-8640.

[5] J. Fan, Z. Shi, M. Lian, H.Li and J. Yin, *J. Mater. Chem. A* , 2013, **1**, 7433-7443.

[6] A. Nakayama, A. Kakugo, J. P. Gong, Y. Osada, M. Takai, T. Erata and S. Kawano, *Adv. Funct. Mater.*, 2004, **14**, 1124-1128.

[7] R. Dash, M. Foston and A. J. Ragauskas, *Carbohydr. Polym.*, 2013, **91**, 638-645.

[8] W. C. Lin, W. Fan, A. Marcellan, D. Hourdet, C. Creton, *Macromolecules*, 2010, **43**, 2554-2563.

[9] K. Haraguchi, *Curr. Opin. Solid State Mater. Sci.* 2007, **11**, 47-54.

[10] L. Xiong, X. Hu, X. Liu, Z. Tong, *Polymer*, 2008, **49**, 5064-5071.

[11] Q. Zhang, X. Li, Y. Zhao, L. Chen, *Appl. Clay Sci.* 2009, **46**, 346-350.

[12] K. S. Novoselov, A. K. Geim, S. V. Morozov, D. Jiang, Y. Zhang, S. V. Dubonos, I. V. Grigorieva, A. A. Firsov, *Science*, 2004, **306**, 666-669.

[13] K. S. Novoselov, A. K. Geim, S. V. Morozov, D. Jiang, M. I. Katsnelson, I. V. Grigorieva, S. V. Dubonos and A. A. Firsov, *Nature*, 2005, **438**, 197-200.

[14] D. A. Dikin, S. Stankovich, E. J. Zimney, R. D. Piner, G. H. B. Dommett, G. Evmenenko, S. T. Nguyen and R. S. Ruoff, *Nature*, 2007, **448**, 457-460.

[15] S. Stankovich, D. A. Dikin, G. H. B. Dommett, K. M. Kohlhaas, E. J. Zimney, E. A. Stach, R. D. Piner, S. T. Nguyen and R. S. Ruoff, *Nature*, 2006, **442**, 282-286.

[16] S. Stankovich, D. A. Dikin, R. D. Piner, K. M. Kohlhaas, A. Kleinhammes, Y. Jia, Y. Wu, S. T. Nguyen and R. S. Ruoff, *Carbon*, 2007, **45**, 1558-1565.

[17] Y. Xu, W. Hong, H. Bai, C. Li, G. Shi, *Carbon*, 2009, **47**, 3538-3543.

[18] J. H. Wu, Q. W. Tang, H. Sun, J. M. Lin, H. Y. Ao, M. L. Huang and Y. F. Huang, *Langmuir,* 2008, **24**, 4800-4805.

[19] W. H. Kai, Y. Hirota, L. Hua, Y. Inoue, *J. Appl. Polym. Sci.*, 2008, **107**, 1395-1400.

[20] Y. X. Xu, Q. Wu, Y. Q. Sun, H. Bai, G. Q. Shi, *ACS Nano*., 2010, **4**, 7358-7362.

[21] M. Kobayashi, Y. S. Chang and M. Oka, *Biomaterials*, 2005, **26**, 3243-3248.

[22] L. Zhang, Z. P. Wang, C. Xu, Y. Li, J. P. Gao, R. Wang and Y. Liu, *J. Mater. Chem.*, 2011, **21**, 10399-10406.

[23] H. Bai, C. Li, X. L. Wang and G. Q. Shi, *Chem. Commun.,* 2010, **46**, 2376-2378.

[24] H. Bai, C. Li, X. L. Wang and G. Q. Shi, *J. Phys. Chem. C*, 2011, **115**, 5545-5551.

[25] J. J. Liang, Y. Huang, L. Zhang, Y. Wang, Y. F. Ma, T. Y. Guo, and Y. S. Chen, *Adv. Funct. Mater.,* 2009, **19**, 2297-2302.

[26] M. J. McAllister, J. L. Li, D. H. Adamson, H. C. Schniepp, A. A. Abdala, J. Liu, M. Herrera-Alonso, D. L. Milius, R. Car, R. K. Prud'homme, I. A. Aksay, *Chem. Mater.,* 2007, **19**, 4396-4404.

[27] S. Stankovich, D. A. Dikin, R. D. Piner, K. A. Kohlhaas, A. Kleinhammes, Y. Jia, Y. Wu, S. T. Nguy en, R. S. Ruoff, *Carbon*, 2007, **45**, 1558-1565.

[28] Y. C. Si, E. T. Samulski, *Nano Lett.,* 2008, **8**, 1679-1682.

[29] W. Gao, L. B. Alemany, L. Ci, P. M. Ajayan, *Nat. Chem.,* 2009, **1**, 403-408.

[30] D. Li, M. B. Müller, S. Gilje, R. B. Kaner, G. G. Wallace, *Nat. Nanotechnol.,* 2008, **3**, 101-105.

[31] L. Q. Liu, A. H. Barber, S. Nuriel, H. D. Wagner, *Adv. Funct. Mater.,* 2005, **15**, 975-980.

[32] S. Song, A. Song and J. Hao, *J. Phys. Chem. B*, 2012, **116**, 12850-12856.

[33] A. Pal, H. Basit, S. Sen, V. Aswal and S. Bhattacharya, *J. Mater. Chem.*, 2009, **19**, 4325-4334.

[34] F. J. Zhang, Z. H. Xu, S. L. Dong, L. Feng, A. X. Song, C. H. Tung and J. C. Hao, *Soft Matter,* 2014, **10**, 4855-4862.

[35] J. Z. Xu, T. Chen, C. L. Yang, Z. M. Li, Y. M. Mao, B. Q. Zeng, B. S. Hsiao, *Macromolecules,* 2010, **43,** 5000-5008.

[36] G. Goncalves, P. A. A. P. Marques, C. M. Granadeiro, H. I. S. Nogueira, M. K. Singh, J. Gracio, *Chem. Mater.,* 2009, **21,** 4796–4802.

[37] K. Jasuja, V. Berry, *ACS Nano*, 2009, **3**, 2358 –2366.

[38] W. G. Tu, Y. Zhou, Z. G. Zou, *Adv. Funct. Mater.* 2013, **23,** 4996–5008.

[39] Y. T. Wang, X. Xin, W. Z. Li, C. Y. Jia, L. Wang, J. L. Shen, G. Y. Xu, *J. Colloid Inter. Sci.*, 2014, **431**, 82-89.

[40] Y. Han,; Y. Lu, *Compos. Sci. Technol.*, 2009, **69**, 1231–1237.

[41] X. M. Yang, Y. F. Tu, L. Li, S. M. Shang, X. M. Tao, *ACS Appl. Mater. Inter.*, 2010, **2**, 1707-1713.

[42] X. F. Sun, X. Xin, N. Tang, L. W. Guo, L. Wang, G. Y. Xu, *J. Phy. Chem. B*, 2014, **118**, 824-832.

[43] K. Y. Foo, B. H. Hameed, *Chem. Eng. J.*, 2012, **203**, 81-87.

[44] L.Q. Ji, X. Bai, L. C. Zhou, H. C. Shi, W. Chen, Z. L. Hua, *Front. Environ. Sci. Eng.* 2013, **7**, 442-450.

[45] L. Ai, C. Zhang, Z. Chen, *J. Hazard. Mater.*, 2011, **192**, 1515–1524.

[46] C. P. Li, M. She, X. D. She, J. Dai, L. X. Kong, *J. Appl. Polym. Sci.*, 2014, **131**, DOI: 10.1002/app.39872.

GE